National Aeronautics and
Space Administration

Jet Propulsion Laboratory
California Institute of Technology
Pasadena, California

Introduction to V6 and V7
and
Recent Science Highlights

Eric J. Fetzer

Jet Propulsion Laboratory / California Institute of Technology

AIRS Science Team Meeting, Greenbelt, MD

November 8-11, 2011

V6 Status

Improvements since V5 include:

- **Reduced spurious cooling trend in the free troposphere.**
- **Smaller temperature biases.**
- **Higher yield**
  - ***No trend in yield.***
- **Improved surface properties (see Glynn Hulley talk).**
- **Improved cloud properties (see Van Dang talk).**
- **Improved trace gases.**

National Aeronautics and Space Administration

Jet Propulsion Laboratory
California Institute of Technology
Pasadena, California

V6 Has Higher Yield and No Yield Trend

Higher Yield

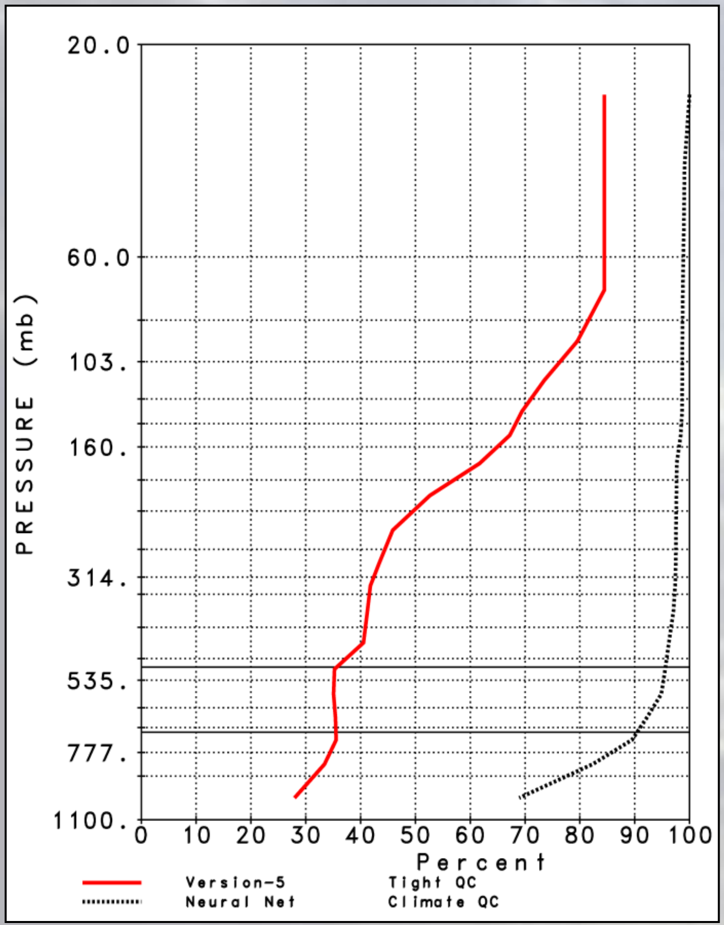

Removed Trend in Yield

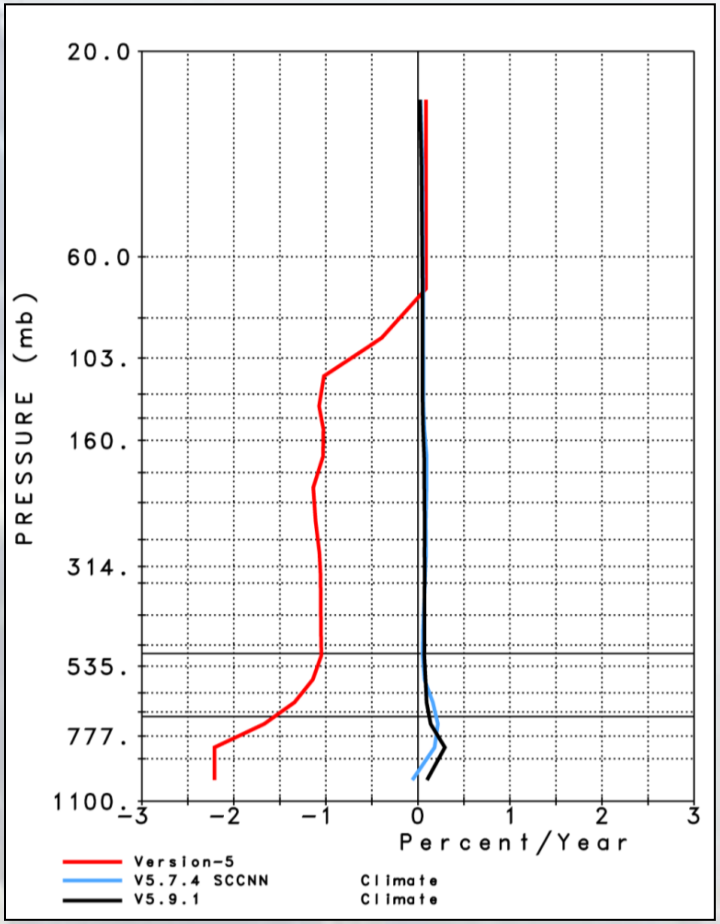

Courtesy J. Susskind, GSFC

National Aeronautics and Space Administration

Jet Propulsion Laboratory
California Institute of Technology
Pasadena, California

Reduced Temperature Trends
Location of radiosondes coincident with AIRS (1 hr and 100 km) SON 2006

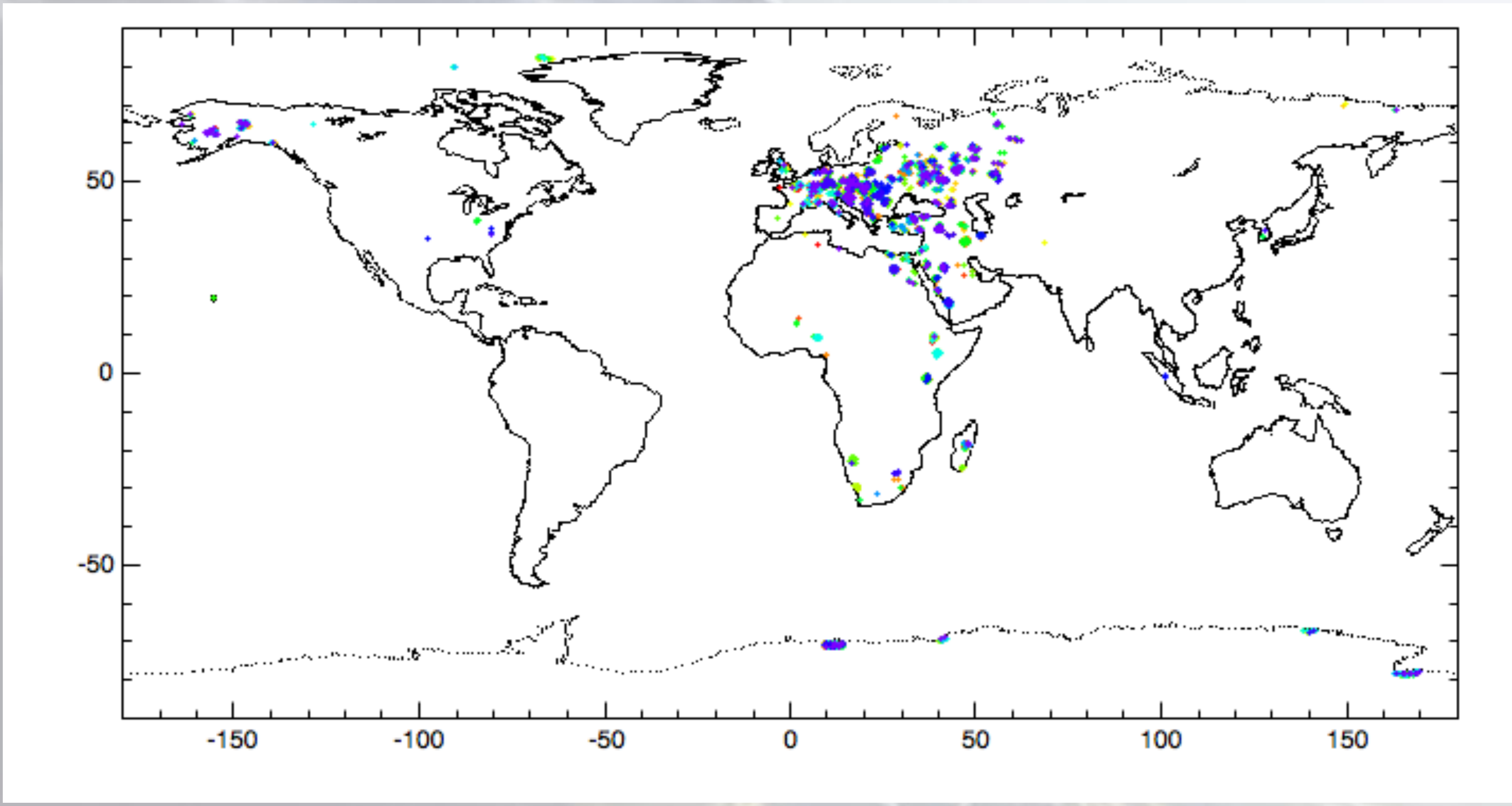

Courtesy F. W. Irion, JPL

National Aeronautics and Space Administration

Jet Propulsion Laboratory
California Institute of Technology
Pasadena, California

Temperature bias results for AIRS – RaObs
V5.0.14 and V5.9.12 30°N – 60°N SON 2006

init – sonde bias

No. of matched observations

final – init bias

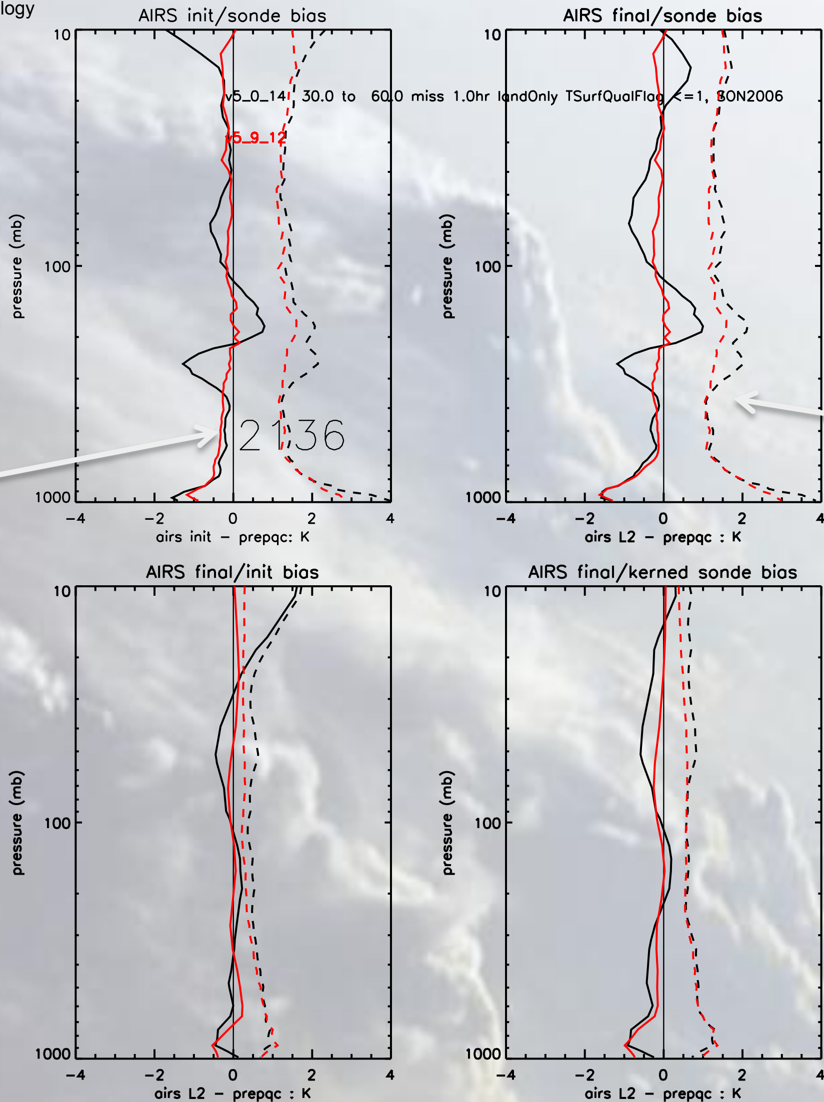

final – sonde bias

RMS

Final – sonde kerned by AIRS averaging kernel

i.e. sonde profile is

$$\hat{x} = x_0 + \mathrm{A}(x_T - x_0)$$

1 hr miss time and 100 km miss distance from sonde launch. Data taken from 1st, 6th, 11th, 16th, 21st and 26th of each month. Data matched one-to-one between versions with both passing qualSurf =0 or 1.

Courtesy F. W. Irion, JPL

National Aeronautics and Space Administration

Jet Propulsion Laboratory
California Institute of Technology
Pasadena, California

Temperature bias trend results for AIRS – RaObs V5.0.14 and V5.9.12 30°N – 60°N

Trend in init - sonde

Trend in final - sonde

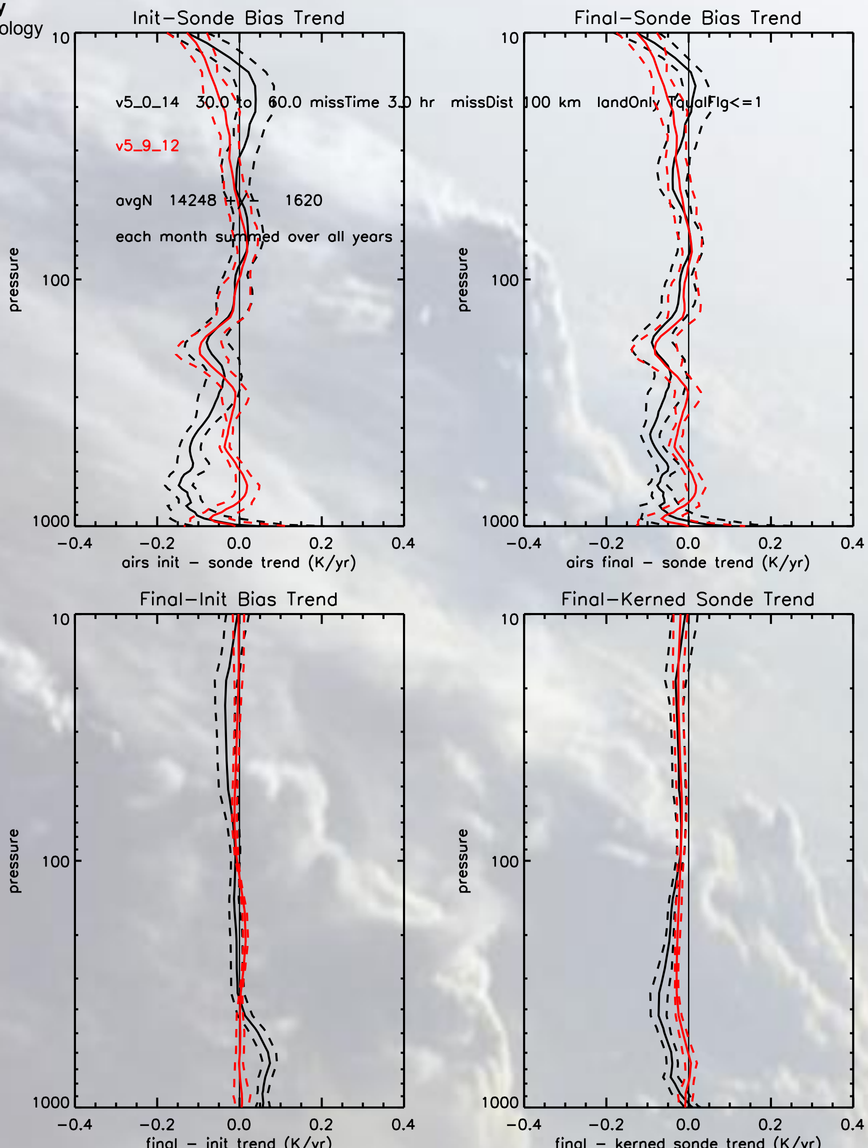

Trend in final - init

Trend in Final – sonde kerned by AIRS averaging kernel

i.e. sonde profile is

$$\hat{x} = x_0 + \mathrm{A}(x_T - x_0)$$

3 hr miss time and 100 km miss distance from sonde launch. Data taken from 1st, 6th, 11th, 16th, 21st and 26th of each month through 2009.

Data matched one-to-one between versions with both passing qualSurf =0 or 1.

Trends calculated by finding linear trends for each calendar month and then averaging.

Improvements in AIRS Cloud Top Properties Compared to V5

Verified by CloudSat/CALIPSO:

- AIRS V5.9.12 is able to detect more clouds.
- More realistic Cloud Top Height for AIRS V5.9.12 -- especially low level clouds.
- AIRS Top Layer Cloud Top Height distribution is not as wildly off in V5.9.12, especially for multilayered clouds.
- Defaulting to NN surface temperature for cloud retrieval gives better CTH comparisons
  - *same cases in V5 did not compare as well.*

Courtesy Van Dang, JPL

National Aeronautics and
Space Administration

Jet Propulsion Laboratory
California Institute of Technology
Pasadena, California

AIRS V6 water vapor is not simply replicating ECMWF

V6 AIRS at 850 hPa

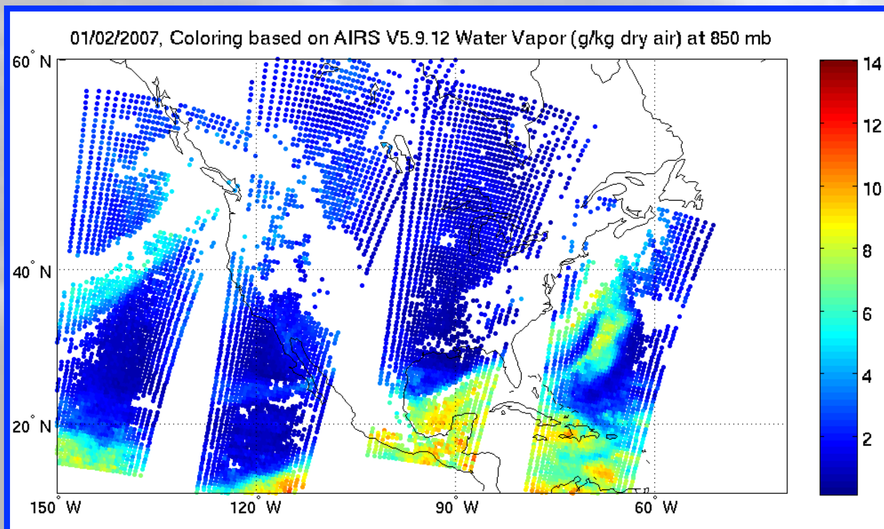

ECMWF at 850 hPa

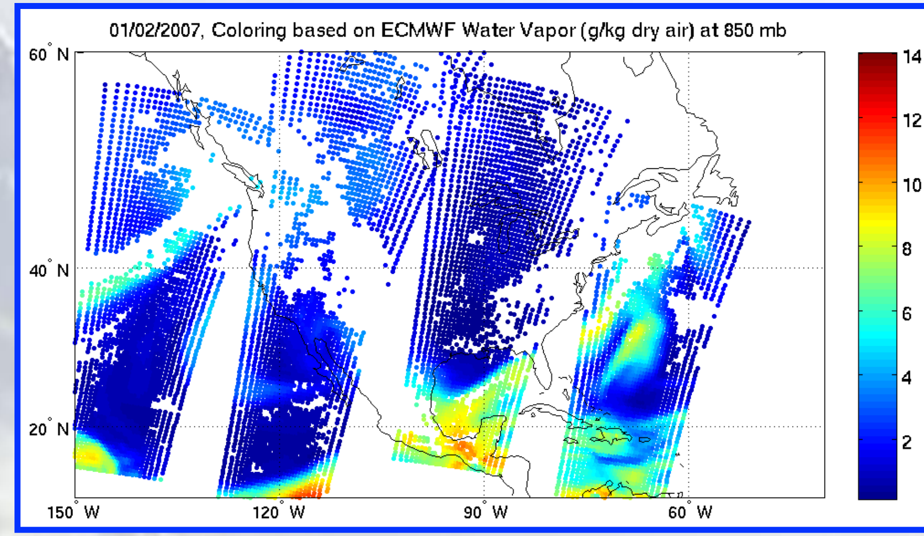

Differences of order ±100%

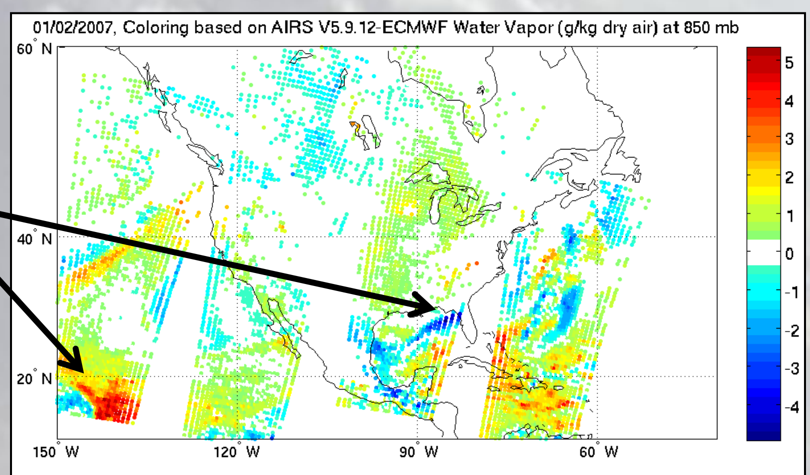

Courtesy Van Dang, JPL

National Aeronautics and
Space Administration

Jet Propulsion Laboratory
California Institute of Technology
Pasadena, California

Next Step: Assessing AIRS relative to other global data sets

We need to ask hard questions like:

- **Has ECMWF become so good it is nearly indistinguishable from AIRS?**
- **Is the neural network replicating ECMWF?**

Apparently "no" to both, but we need metrics to answer these and similar questions.

- ***How different are they?***
- ***Where and why?***

One Motivation: Boundary Layer Science

- **How much additional information is in the boundary layer?**
  - ***We know V5 is informative, but V6 is better.***

- **We should do better than models over land**
  - ***Assimilated microwave radiances provide limited information here, and near-surface IR is not fully assimilated because of clouds.***

National Aeronautics and Space Administration
Jet Propulsion Laboratory
California Institute of Technology
Pasadena, California

Another Motivation: Climate Trends

- **What are the trends in important climate variables like water vapor, clouds, trace gases (and yes, temperature).**
  - ***The AIRS record is becoming long enough to reach some robust conclusions about climate processes.***

Decadal trend in TPW

Santer et al. (2007), Identification of human-induced changes in atmospheric moisture content, *PNAS*.

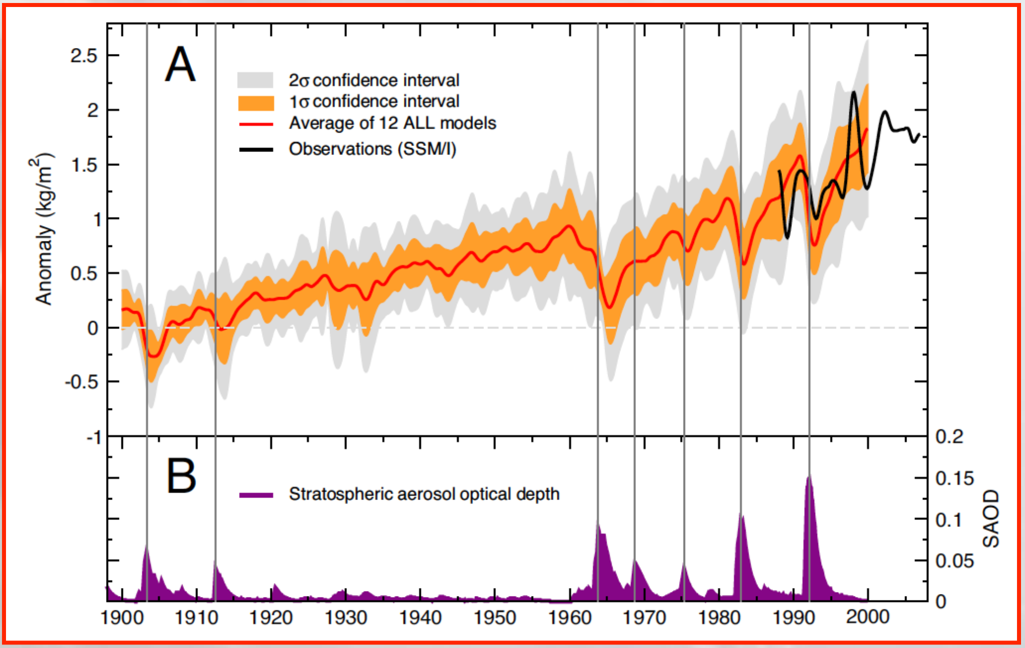

What to expect in V7

- **Better selection of water vapor channels from Antonia Gambacorta.**

- **Better information content analysis.**

National Aeronautics and
Space Administration

Jet Propulsion Laboratory
California Institute of Technology
Pasadena, California

AIRS Key Products and Science Areas

CO

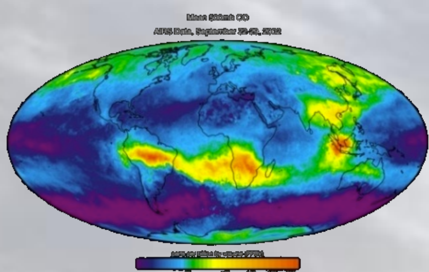

Cloud and Water Vapor Processes

Atmospheric Temperature

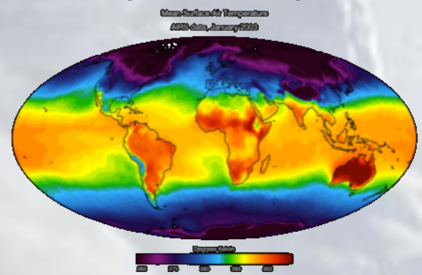

Cloud Properties

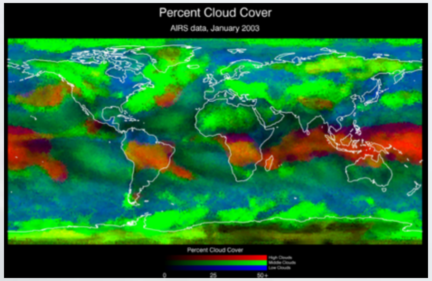

Greenhouse Gas Forcing

Ozone

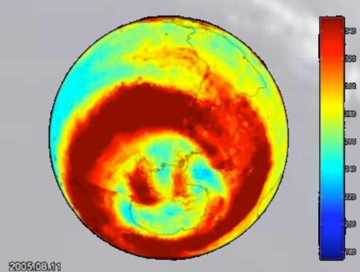

Atmospheric Water Vapor

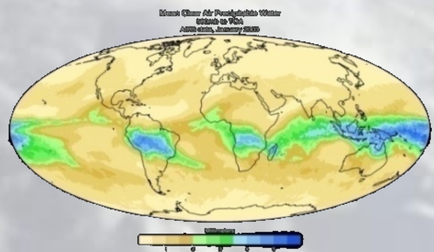

Dust

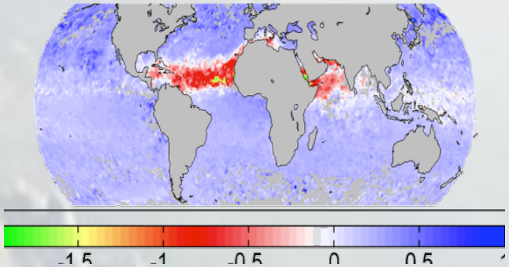

Methane

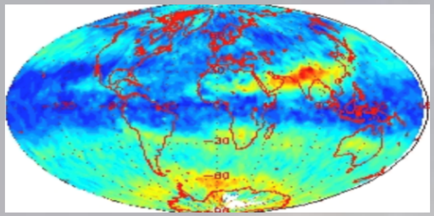

CO2

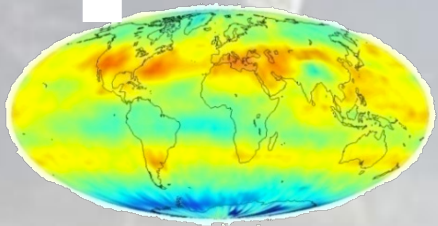

SO2

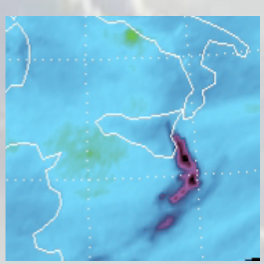

Emissivity

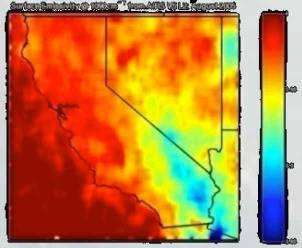

National Aeronautics and
Space Administration

Jet Propulsion Laboratory
California Institute of Technology
Pasadena, California

440 AIRS Peer Reviewed Publications to Date

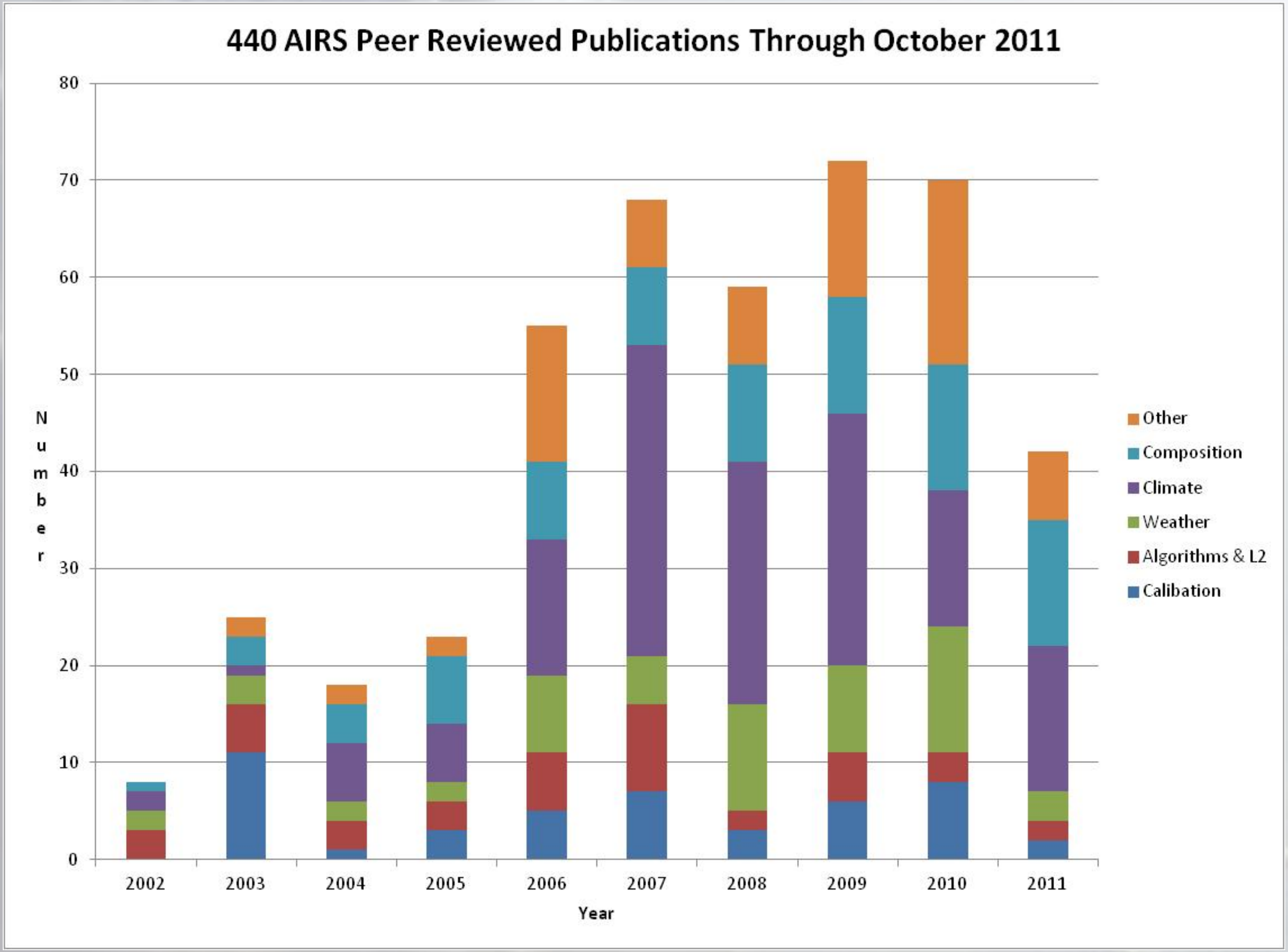

AIRS CO_2 Constraining Chemistry Models

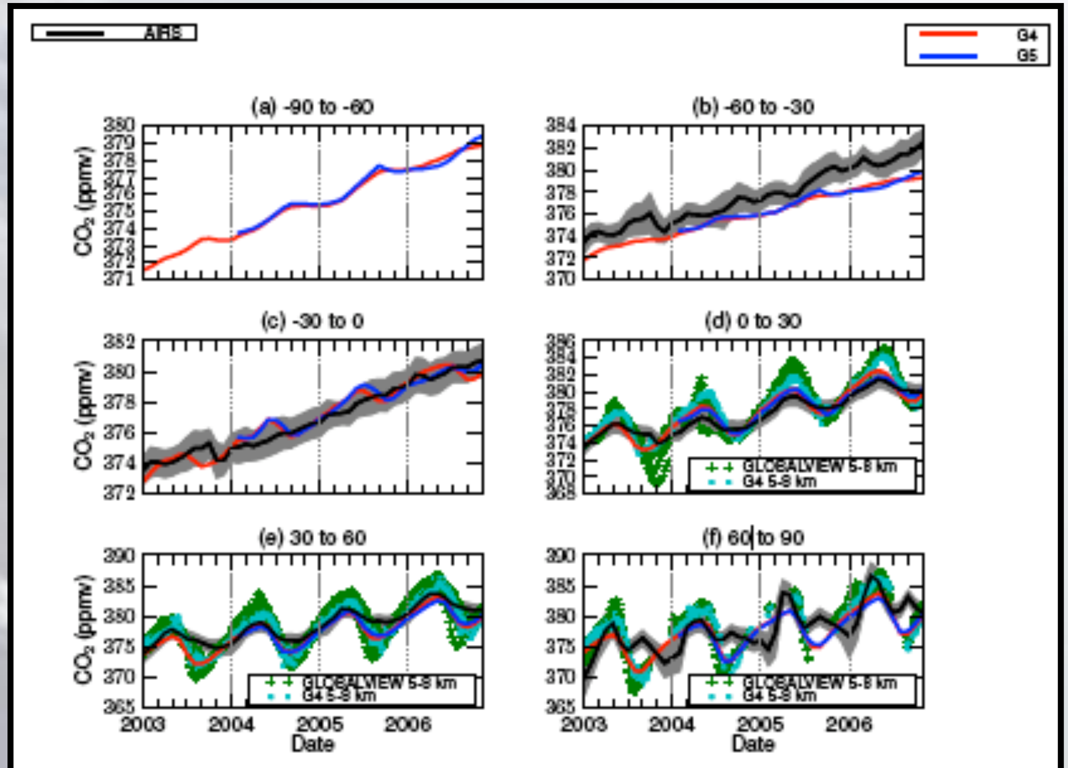

Monthly-mean AIRS (black) and a posteriori model (red GEOS-4 and blue GEOS-5) CO2 concentrations (ppm) averaged over 30 degree latitude bins during 2003–2006: (a) 60 S–90 S, (b) 30 S–60 S, (c) 0–30 S, (d) 0–30 N, (e) 30 N–60 N, and (f) 60 N–90 N. The GEOS-Chem model, described at a horizontal resolution of 2 ° 2.5, has been sampled at the time and location of each AIRS level-3 CO2 scene, weighted by the observation numbers, and convolved using the vertical weighting functions from Chahine et al. (2008).

Feng, L., Palmer, P. I., Yang, Y., Yantosca, R. M., Kawa, S. R., Paris, J.-D., Matsueda, H., and Machida, T.: Evaluating a 3-D transport model of atmospheric CO_2 using ground-based, aircraft, and space-borne data, *Atmos. Chem. Phys., 11,* 2789-2803, doi:10.5194/acp-11-2789-2011, 2011.

National Aeronautics and
Space Administration

Jet Propulsion Laboratory
California Institute of Technology
Pasadena, California

Observations of Deep Convective Clouds

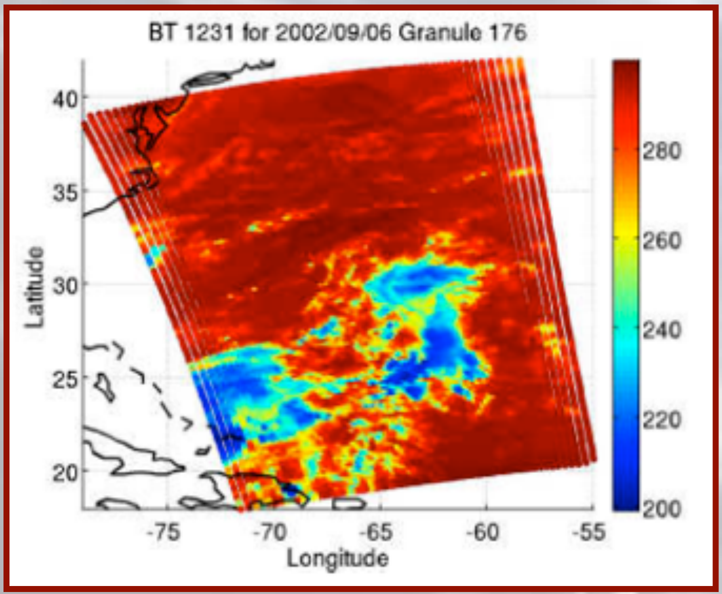

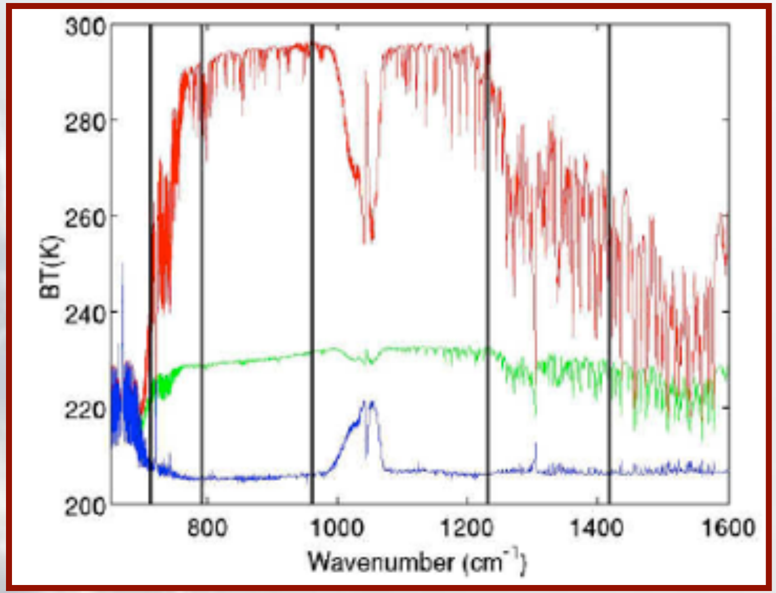

Aumann, H. H., DeSouza-Machado, S. G., and Behrangi, A.: Deep convective clouds at the tropopause, *Atmos. Chem. Phys., 11,* 1167-1176, doi:10.5194/acp-11-1167-2011, 2011.

National Aeronautics and Space Administration

Jet Propulsion Laboratory
California Institute of Technology
Pasadena, California

AIRS and MLS give complete picture of atmospheric water vapor

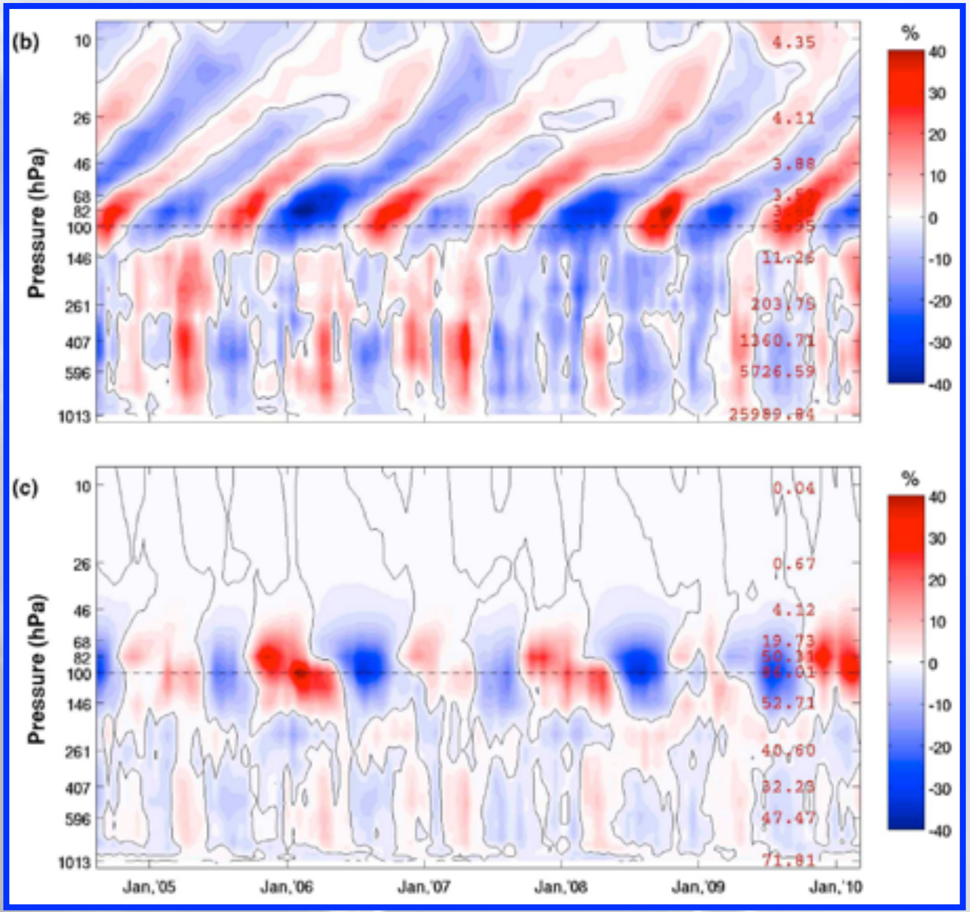

Equatorial mean (08°S–08°N, 180°E–180°W) time evolution of (b) water vapor (%), and (c) RH (%) with the time record mean removed at each pressure level.

Liang, C. K., A. Eldering, A. Gettelman, B. Tian, S. Wong, E. J. Fetzer, and K. N. Liou (2011), Record of tropical interannual variability of temperature and water vapor from a combined AIRS-MLS data set, *J. Geophys. Res., 116,* D06103, doi:10.1029/2010JD014841.

National Aeronautics and Space Administration

Jet Propulsion Laboratory
California Institute of Technology
Pasadena, California

AIRS Validates Upper Tropospheric Water Vapor and Temperature in Models

Weather and climate model upper tropospheric water vapor and temperature.

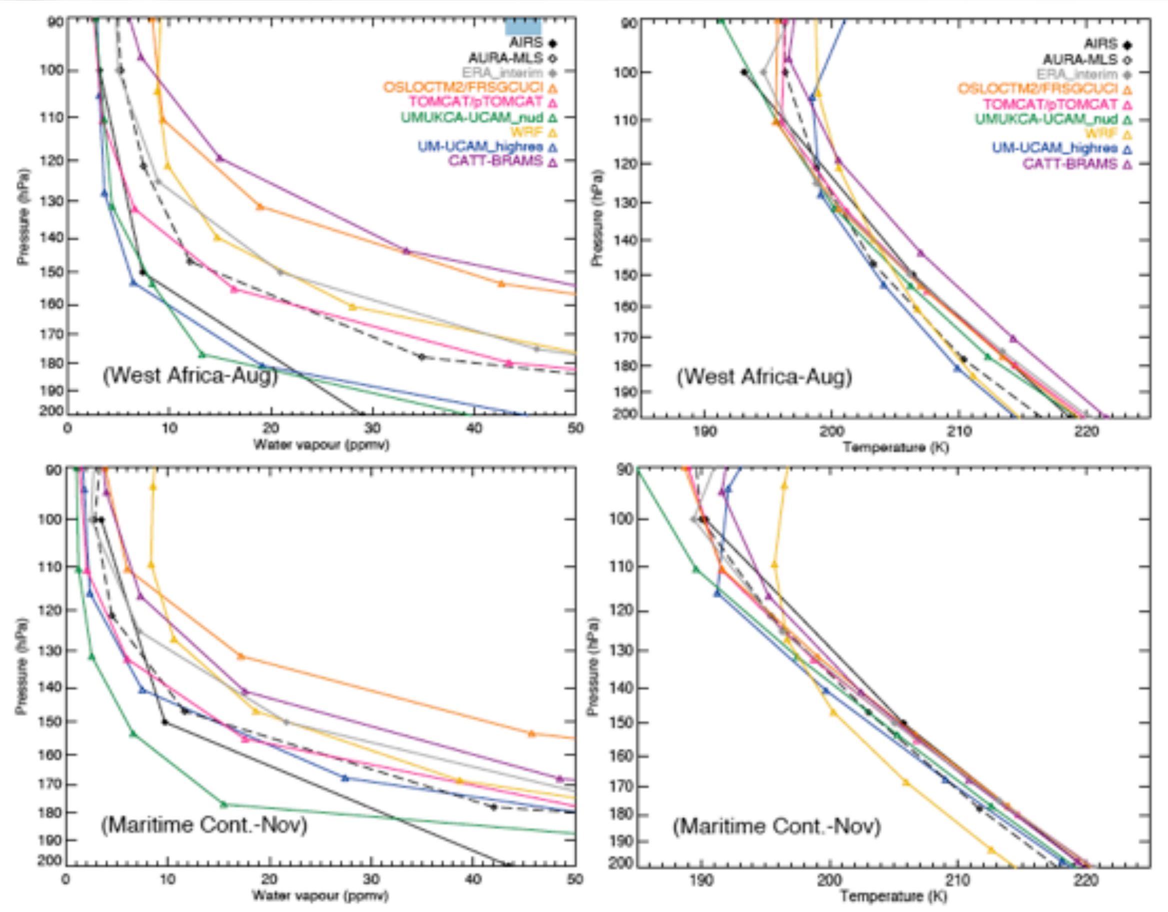

Russo, M. R., Marécal, V., Hoyle, C. R., Arteta, J., Chemel, C., Chipperfield, M. P., Dessens, O., Feng, W., Hosking, J. S., Telford, P. J., Wild, O., Yang, X., and Pyle, J. A.: Representation of tropical deep convection in atmospheric models – Part 1: Meteorology and comparison with satellite observations, *Atmos. Chem. Phys., 11,* 2765-2786, doi:10.5194/acp-11-2765-2011, 2011.

National Aeronautics and Space Administration

Jet Propulsion Laboratory
California Institute of Technology
Pasadena, California

Temperature Inversions and Winter Sea Ice

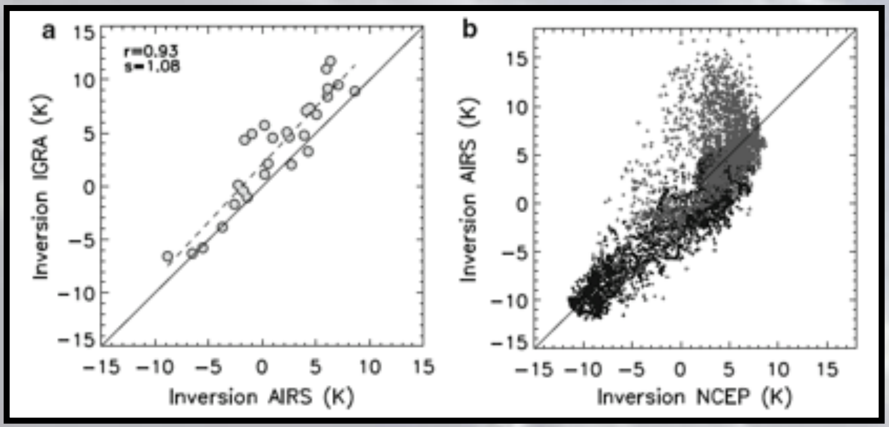

AIRS inversions well validated with radiosondes.

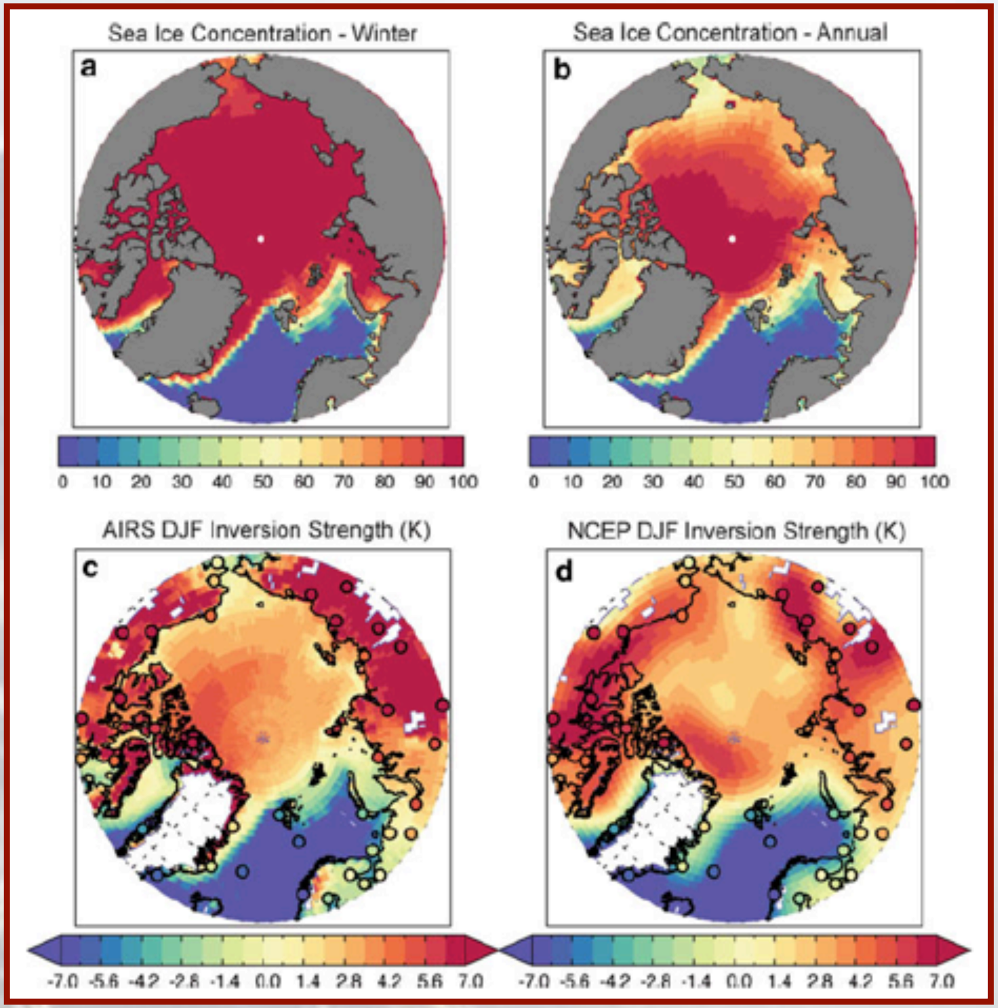

Sea Ice (top) and Inversions (Bottom)

Pavelsky, T., J. Boé, A. Hall, E. J. Fetzer (2011), Atmospheric inversion strength over polar oceans in winter regulated by sea ice, *Clim. Dyn.*, *36*, 945–955.

National Aeronautics and Space Administration

Jet Propulsion Laboratory
California Institute of Technology
Pasadena, California

Observations of air-sea interactions over ocean fronts

AMSR-E SST Laplacian

AIRS thickness (850-1000 hPa) Laplacian

QuikSCAT wind Laplacian

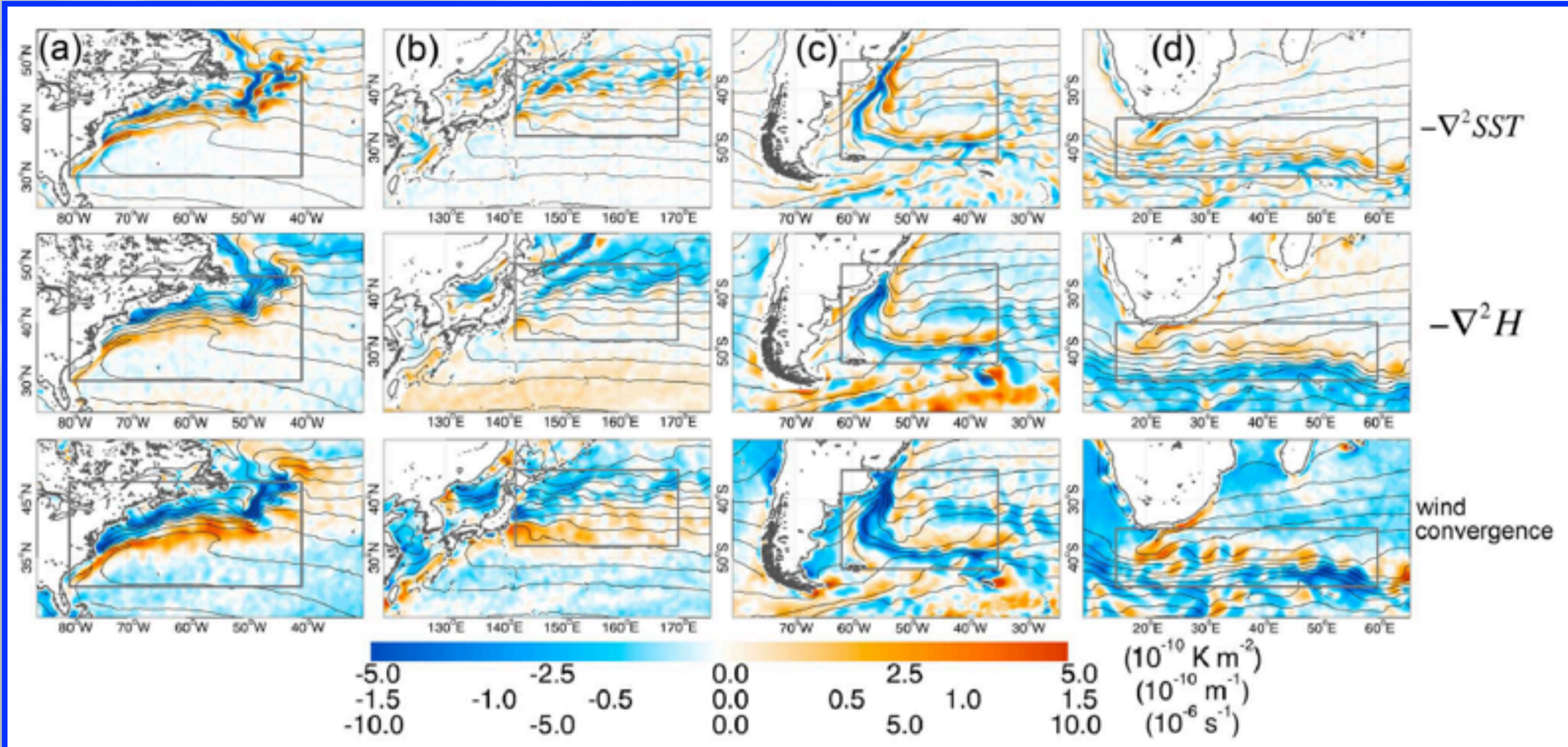

Shimada, T., and S. Minobe (2011), Global analysis of the pressure adjustment mechanism over sea surface temperature fronts using AIRS/Aqua data, *Geophys. Res. Lett., 38,* L06704, doi:10.1029/2010GL046625.

National Aeronautics and Space Administration

Jet Propulsion Laboratory
California Institute of Technology
Pasadena, California

Marine Boundary Layer Clouds and Lower Tropospheric Stability as Observed by AIRS and CloudSat

Observations and models agree well in three areas where CloudSat detects frequent low clouds, but AIRS has infrequent retrievals. Poorer agreement in N. Atlantic suggests issues with representativeness of AIRS retrievals.

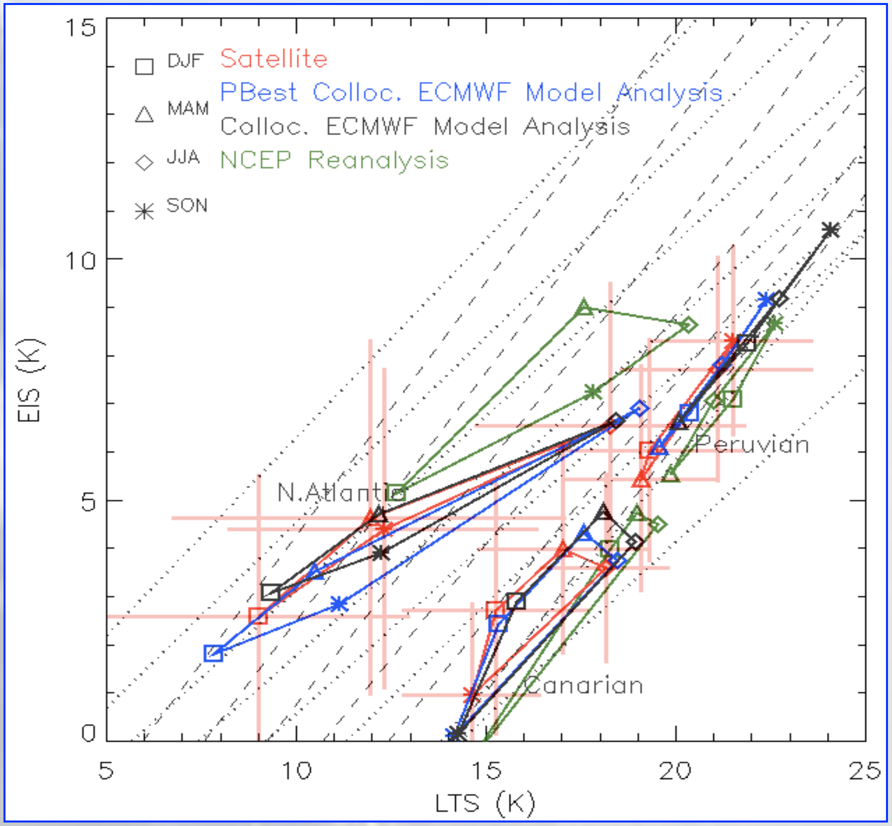

Yue, Q. B. H. Kahn, E. J. Fetzer, and J. Teixeira (2011), Relationship between marine boundary layer clouds and lower tropospheric stability observed by AIRS, CloudSat and CALIOP, J . *Geophys. Res., in press.*

National Aeronautics and Space Administration

Jet Propulsion Laboratory
California Institute of Technology
Pasadena, California

AIRS Reveals Relative Humidity in the Presence of Hurricane Isabel

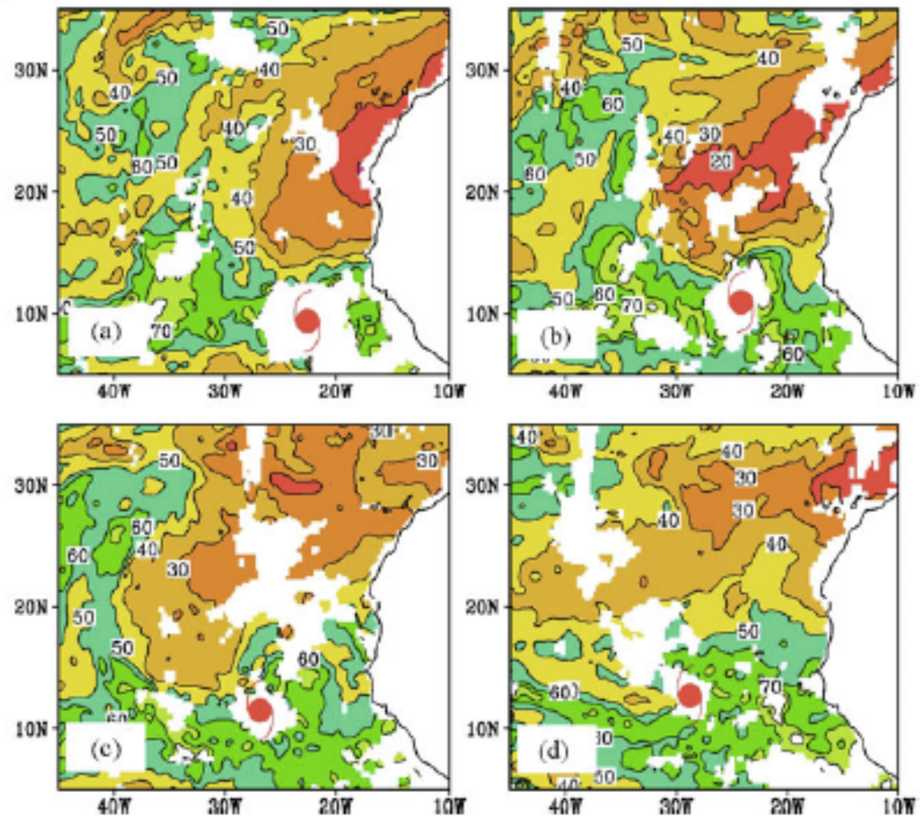

Fig. 10. The 850-hPa relative humidity field derived from the AIRS suite for (a) 2 Sep, (b) 3 Sep, (c) 4 Sep, and (d) 5 Sep 2003. The hurricane symbol indicates the locations of the tropical disturbance, which became Hurricane Isabel on 7 Sep 2003.

Pan, W. Y., L. G. Wu, and C.-L. Shie, 2011: Influence of the Saharan Air Layer on Atlantic tropical cyclone formation during the period 1–12 September 2003, *Adv. Atmos. Sci., 28(1),* 16–32, doi: 10.1007/s00376-010-9165-5.

AIRS Humidity Used to Constrain Cirrus Cloud Trajectory Model

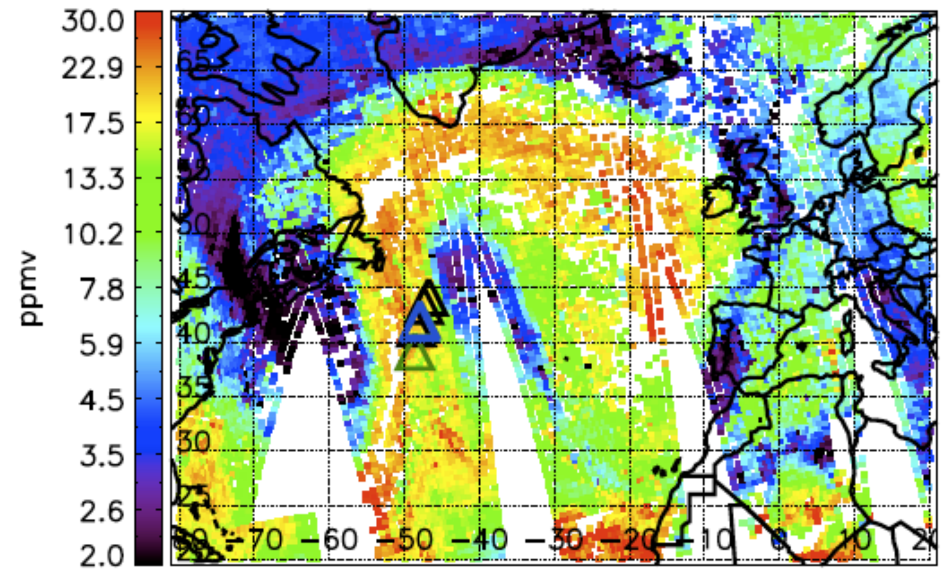

Figure 3. AIRS water vapor mixing ratios measured on 16 January 2006 from 0600 to 1800 UTC in the 150–200 pressure layer. Triangles indicate the locations of the computed 340 K (black), 341 K (blue), and 342 K (green) (~185/194 hPa) back trajectories on 16 January 2006 at 1200 UTC.

Montoux, N., P. Keckhut, A. Hauchecorne, J. Jumelet, H. Brogniez, and C. David (2010), Isentropic modeling of a cirrus cloud event observed in the midlatitude upper troposphere and lower stratosphere, J. Geophys. Res., 115, D02202, doi:10.1029/2009JD011981.

National Aeronautics and Space Administration

Jet Propulsion Laboratory
California Institute of Technology
Pasadena, California

AIRS Radiances Validate Clouds in Forecast Model

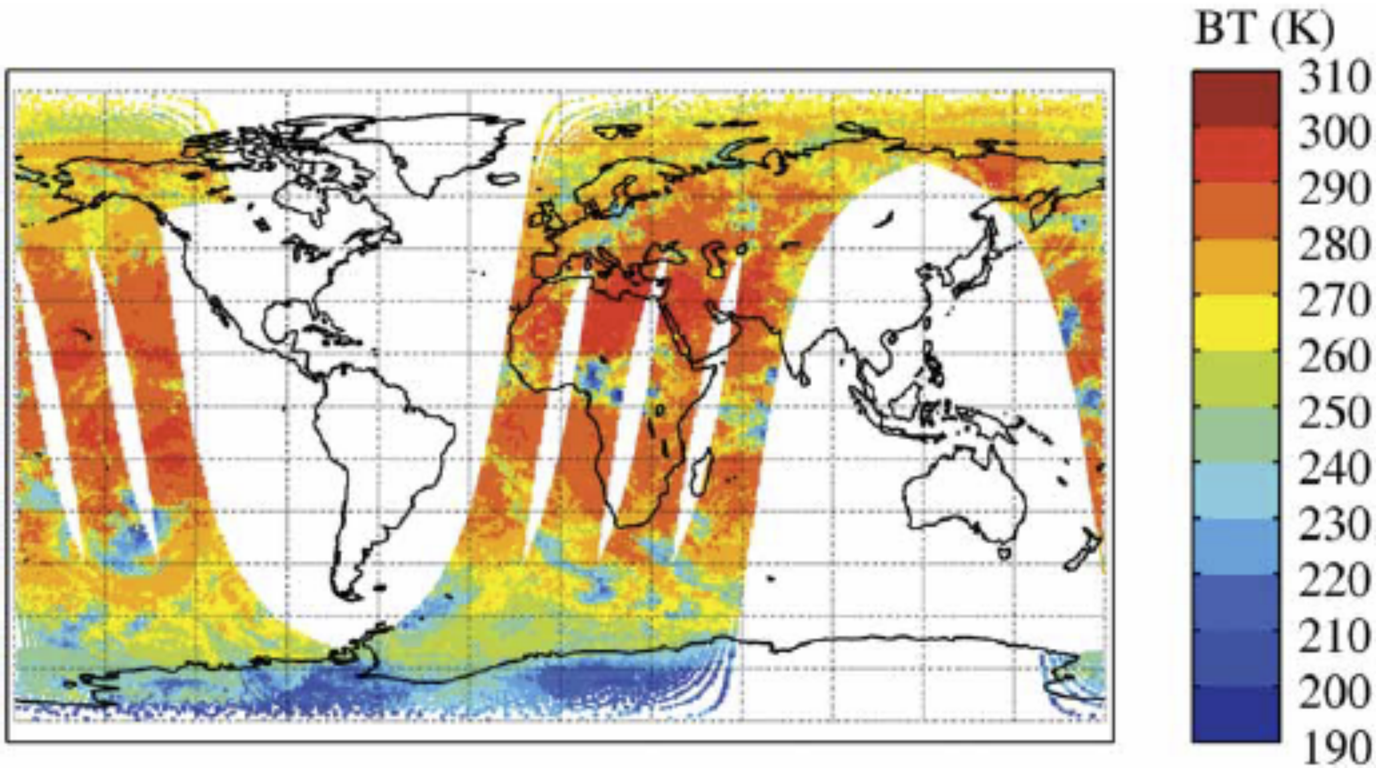

Fig. 1 AIRS channel 787 (10.9 μm) observed brightness temperature (K) for the 6 h period centred on 14 July 2008, 00:00 GMT.

Garand, L., O. Pancrati and S. Heilliette (2011): Validation of forecast cloud parameters from multispectral AIRS radiances, *Atmosphere-Ocean,* 49:2, 121-137

National Aeronautics and Space Administration

Jet Propulsion Laboratory
California Institute of Technology
Pasadena, California

AIRS and MODIS Clouds Are Radiatively Consistent

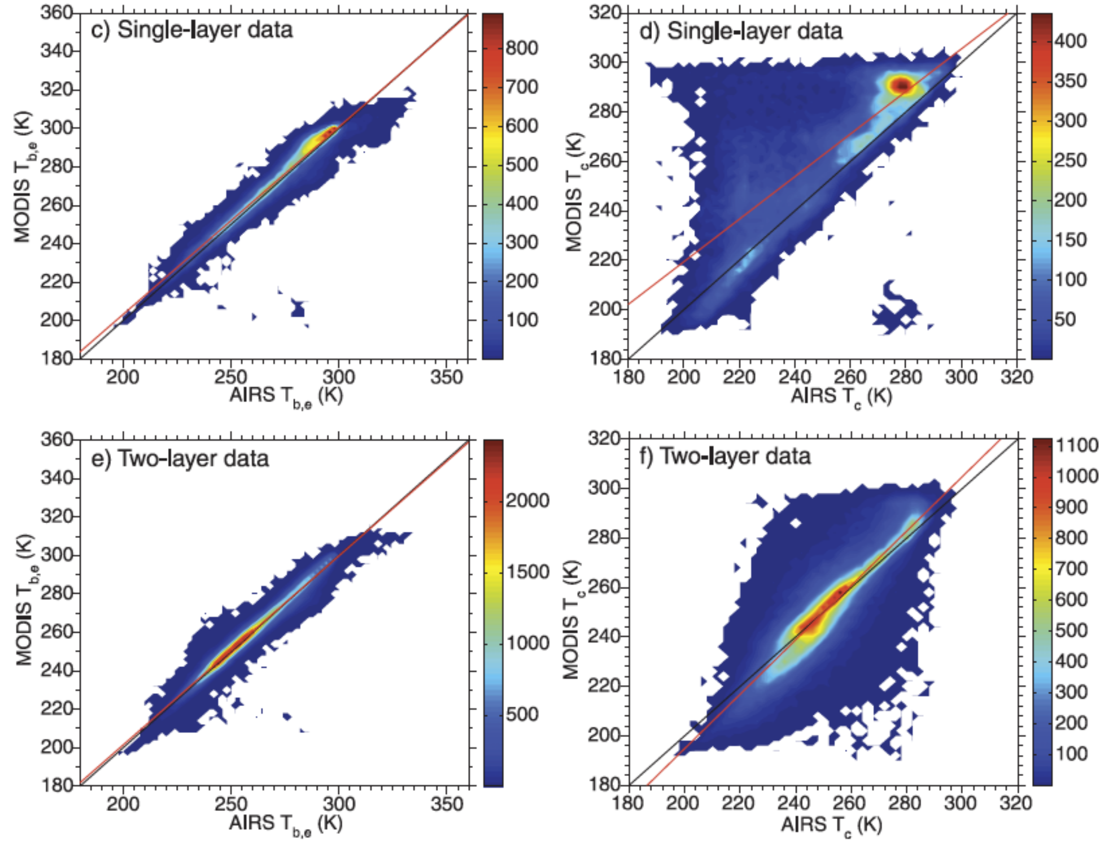

FIG. 1. Comparisons between retrieved MODIS and AIRS (left) effective brightness temperature and (right) cloud-top temperature for 1 Jan 2005. The color scale indicates the number of observations. The 1-to-1 line is shown in black, and the line of best fit is in red. The (a),(b) all-observations, (c),(d) single-layer, and (e),(f) two-layer data are based on AIRS effective cloud fraction as described in the text.

Nasiri, S., V. T. Dang, B. H. Kahn, E. J. Fetzer, M. Schreier (2010), Comparisons of collection 5 MODIS and version 5 AIRS cloud top pressure, cloud fraction, and effective brightness temperature, *J. Applied Met. Clim., 50,* DOI: 10.1175/2010JAMC.

National Aeronautics and Space Administration

Jet Propulsion Laboratory
California Institute of Technology
Pasadena, California

Models and Reanalyses Do Not Replicate AIRS Temperature and Water Vapor Variability

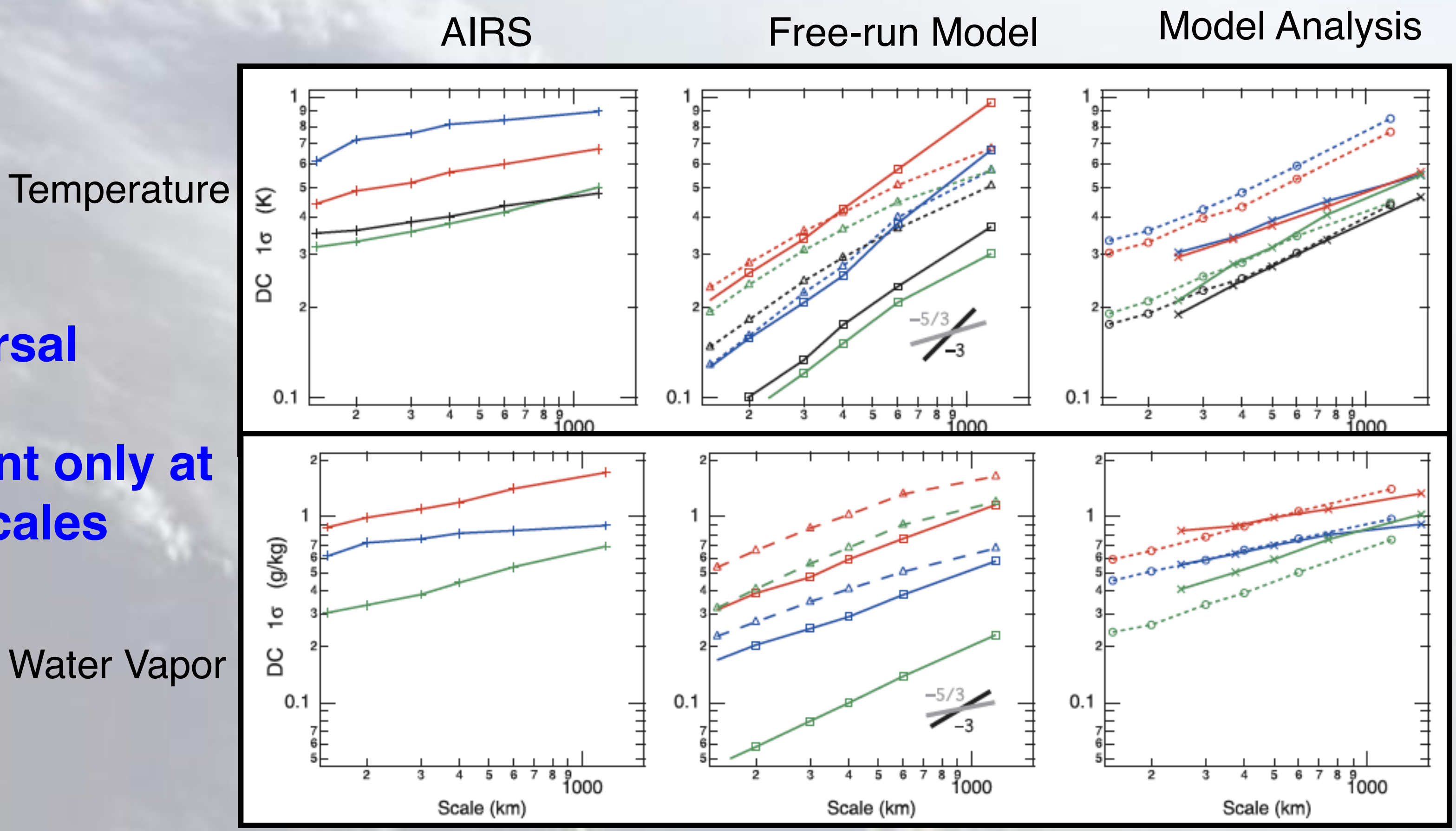

- **No universal structure**
- **Agreement only at largest scales**

Kahn, B. H., J. Teixeira, E. J. Fetzer, A. Gettelman, S. M. Hristova-Veleva, X. Huang, A. K. Kochanski, M. Köhler, S. K. Krueger, R. Wood, and M. Zhao (2011), Temperature and water vapor variance scaling in global models: Comparisons to satellite and aircraft data, *J. Atmos. Sci., 68*, 2156-2168.

National Aeronautics and Space Administration

Jet Propulsion Laboratory
California Institute of Technology
Pasadena, California

Closing the Water Mass Balance with AIRS, MERRA and TRMM

Total atmospheric water mass flux converge from AIRS humidity and MERRA winds.

Surface mass balance from TRMM precipitation and MERRA evaporation.

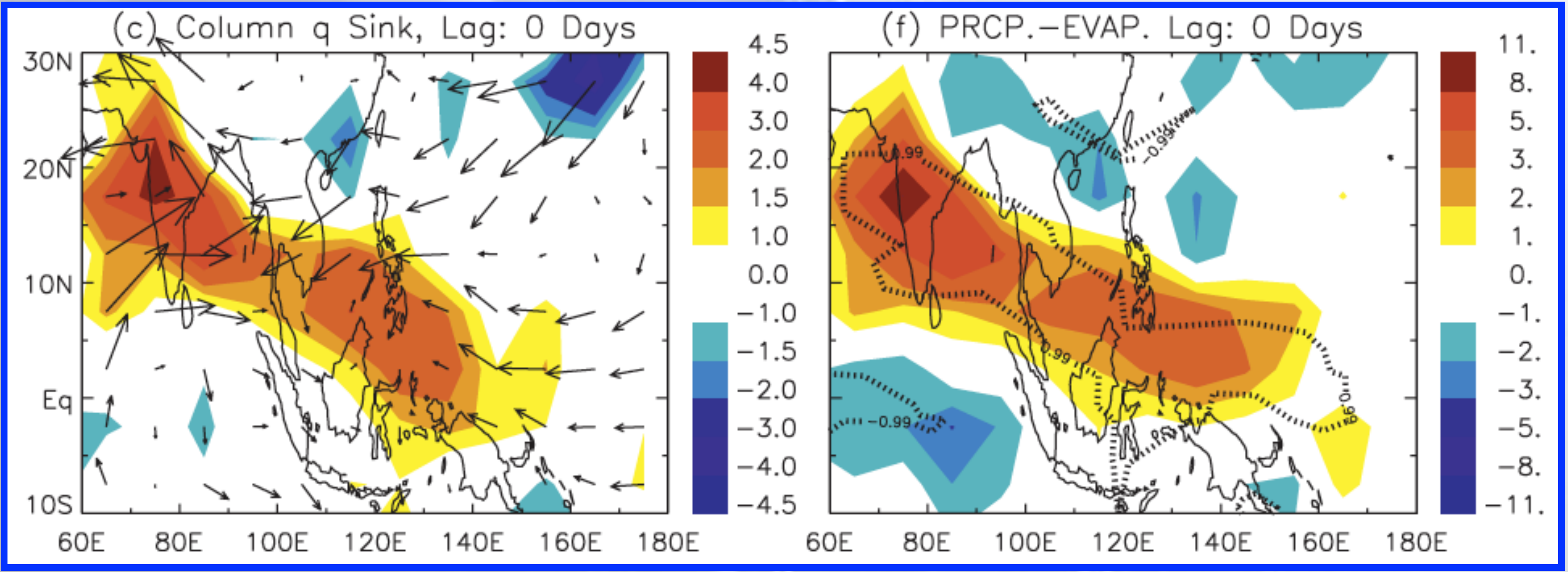

Wong, S., E. J. Fetzer, B. Tian, and B. Lambrigtsen (2011), The apparent water vapor sinks and heat sources associated with the Intraseasonal Oscillation of the Indian Summer Monsoon, *J. Clim., 24,* 4466- 4479.

National Aeronautics and
Space Administration

Jet Propulsion Laboratory
California Institute of Technology
Pasadena, California

Study of Tropical Anvil Clouds

Asymmetry in observed cloud top temperatures

Top: Likely viewing geometry.
Bottom: CloudSat liquid water

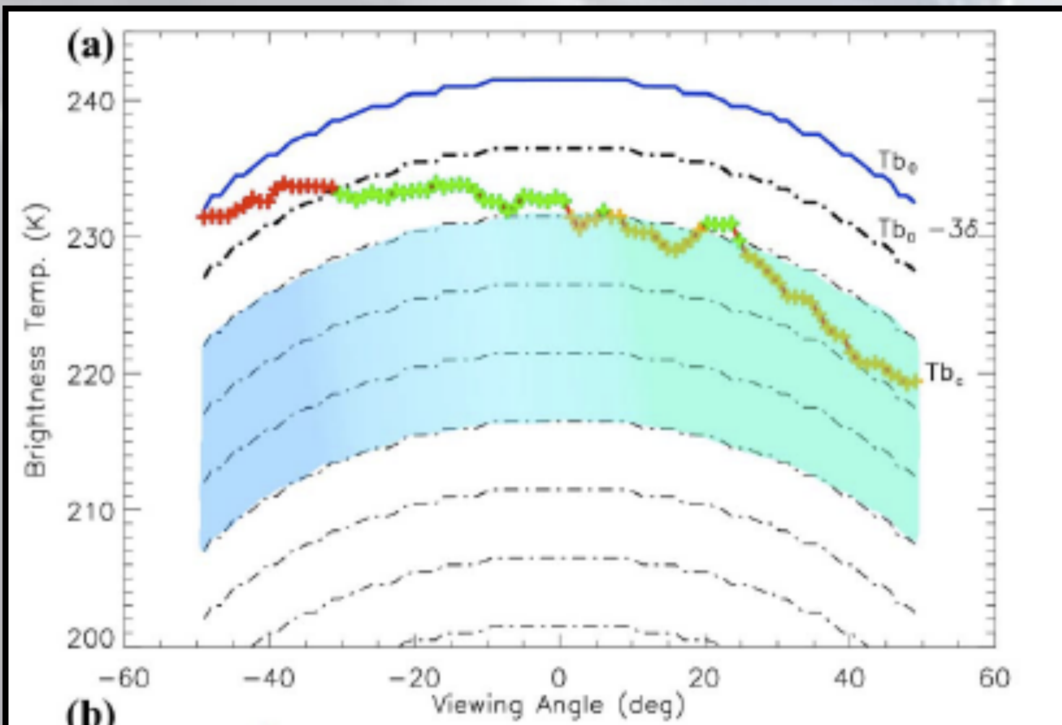

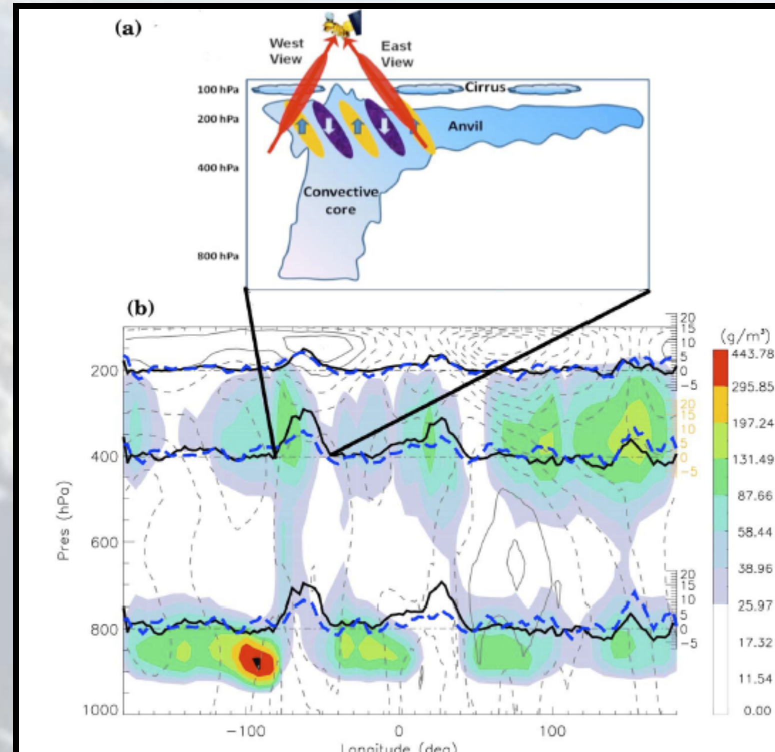

Gong, J., and D. L. Wu (2011), View-angle dependent AIRS cloud radiances: Implications for tropical anvil structures, *Geophys. Res. Lett., 38*, L14802, doi:10.1029/2011GL047910.

National Aeronautics and
Space Administration

Jet Propulsion Laboratory
California Institute of Technology
Pasadena, California

Water Vapor (and Temperature) Inversions in the Arctic Boundary Layer

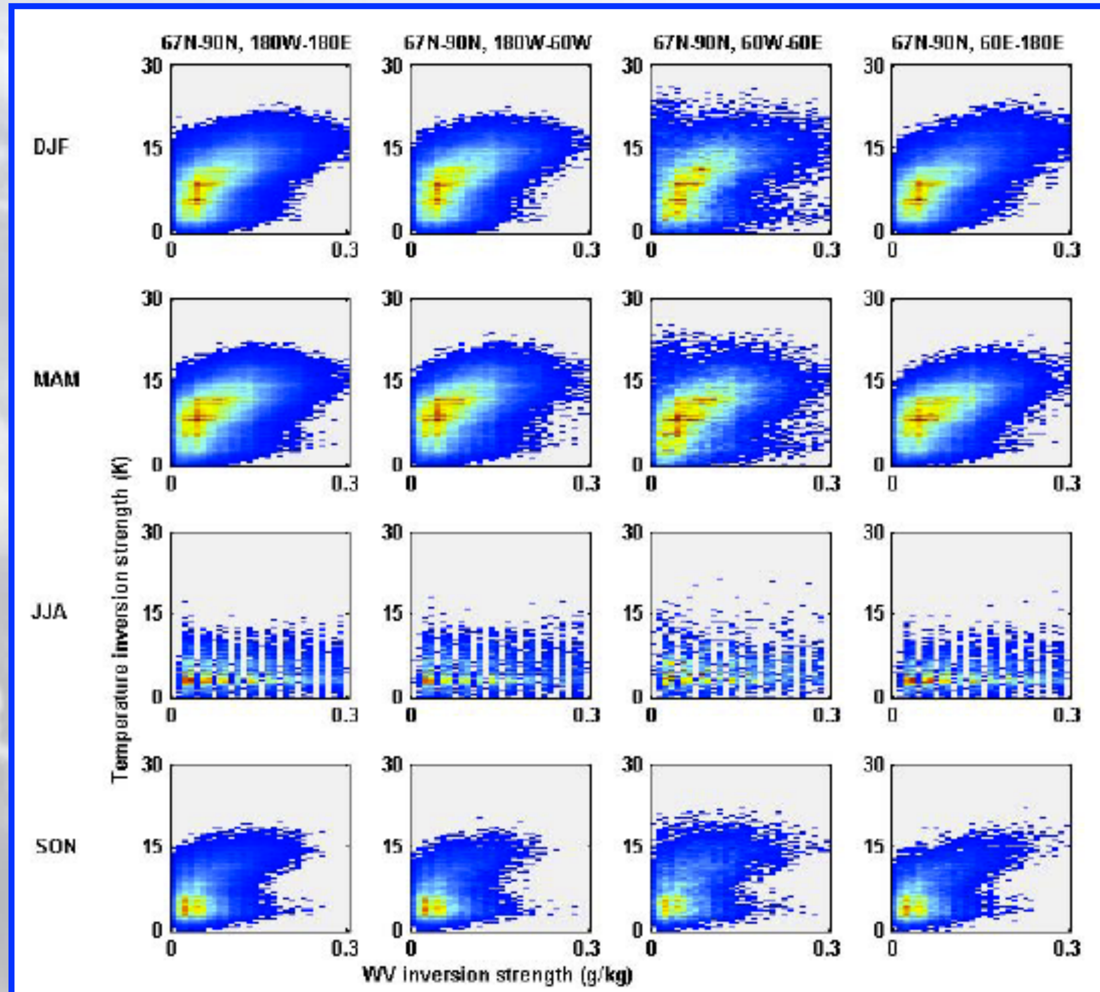

Seasonal frequency, spatial distribution, sampling rates and temperature-humidity inversion covariability (right) from eight years of data determine polar energy balance and are important constraints on model physics.

Devasthale, A., Sedlar, J., and Tjernström, M.: Characteristics of water-vapour inversions observed over the Arctic by Atmospheric Infrared Sounder (AIRS) and radiosondes, *Atmos. Chem. Phys., 11,* 9813-9823, doi:10.5194/acp-11-9813-2011, 2011

National Aeronautics and Space Administration

Jet Propulsion Laboratory
California Institute of Technology
Pasadena, California

Two Studies of 2010 Russian Wildfire Carbon Monoxide

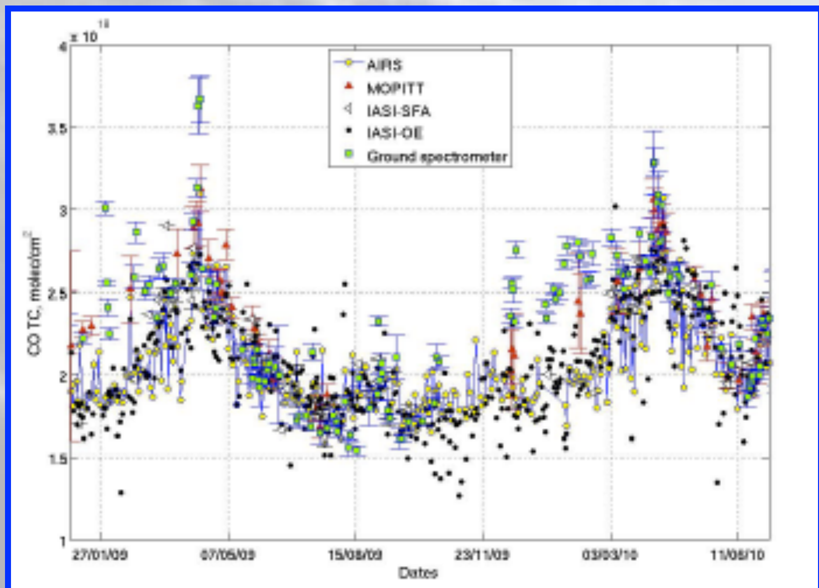

CO time series at 55 N, 37 E, from Yurganov et al.

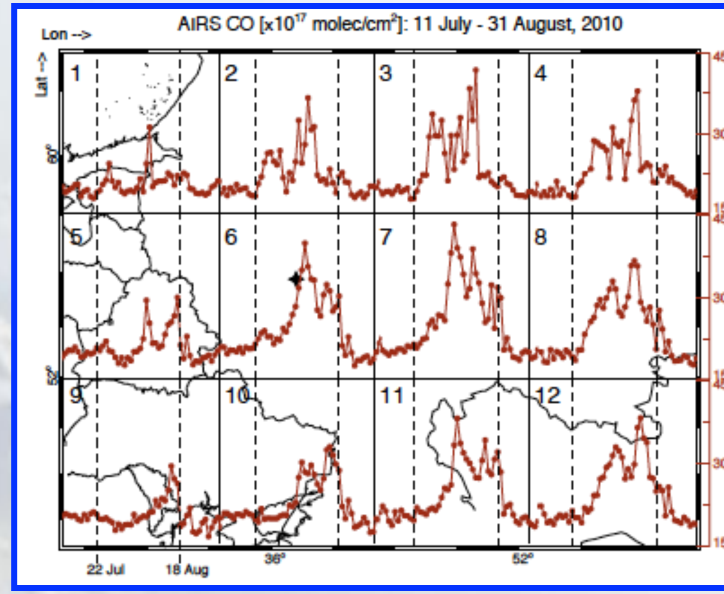

CO time series at three locations over Russia, from Witte et al.

Witte, J. C., Douglass, A. R., da Silva, A., Torres, O., Levy, R. C., and Duncan, B. N.: NASA A-Train and Terra observations of the 2010 Russian wildfires, *Atmos. Chem. Phys. Discuss., 11*, 19113-19142, doi: 10.5194/acpd-11-19113-2011, 2011.

Yurganov, L. N., Rakitin, V., Dzhola, A., August, T., Fokeeva, E., George, M., Gorchakov, G., Grechko, E., Hannon, S., Karpov, A., Ott, L., Semutnikova, E., Shumsky, R., and Strow, L.: Satellite- and ground-based CO total column observations over 2010 Russian fires: accuracy of top-down estimates based on thermal IR satellite data, *Atmos. Chem. Phys., 11*, 7925-7942, doi:10.5194/acp-11-7925-2011, 2011.